Am J Transl Res 2021;13(11):12375-12385
www.ajtr.org /ISSN:1943-8141/AJTR0135458

Original Article

Up-regulation of TUG1 can regulate miR-494/PDK4 axis to inhibit LPS-induced acute lung injury caused by sepsis

Lin Yang, Li Zhao, Hui Zhang, Peili Chen

Department of Critical Care Medicine, The First People's Hospital of Shangqiu, Shangqiu 476100, Henan Province, China

Received May 20, 2021; Accepted September 5, 2021; Epub November 15, 2021; Published November 30, 2021

Abstract: Background: Acute lung injury (ALI) caused by sepsis is the most common disease and the leading cause of death in intensive care units. Recent studies have revealed that long non-coding RNAs (LncRNAs) are abnormally expressed in sepsis. This study aimed to clarify the role and mechanism of Taurine up-regulated gene 1 (TUG1) in ALI caused by sepsis. Methods: Lipopolysaccharide (LPS) was used to simulate sepsis-induced ALI model. RT-PCR, Dual luciferase reporter (DLR) assay and RNA immunoprecipitation (RIP) were used to detect TUG1 and miR-494. The rat model with sepsis-induced ALI was established by intraperitoneal injection of LPS to verify the results of *in vitro* experiments. Results: The expressions of TUG1 and PDK4 were down-regulated while the expression of miR-494 was up-regulated in lung tissues and human small airway epithelial cells (HSAECs). TUG1 was indirectly mediated. Overexpression of TUG1 or inhibition of miR-494 could significantly improve the survival rate of HSAECs. Transfection of miR-494 mimics achieved the opposite effect. Enzyme-linked immunosorbent assay (ELISA) showed that the expression of arthritis-related factors in rats was increased after up-regulating TUG1. Conclusion: TUG1 is lowly expressed in sepsis. Up-regulating TUG1 can alleviate the inflammatory response in ALI caused by LPS-induced sepsis, which may be a clinical treatment target.

Keywords: lncRNA TUG1, miR-494, PDK4, sepsis, acute lung injury

Introduction

Sepsis is an infectious disease caused by pathogens [1]. Infections are usually associated with immune overreaction, which directly endangers the health and life of patients [2]. Sepsis also leads to a series of complications, among which sepsis-induced acute lung injury (ALI) is the major one in clinic [3, 4]. In sepsis-induced ALI, severe inflammation and alterations in apoptosis pathways related proteins result in the destruction of alveolar epithelial cells, which in turn increases epithelial permeability and the inflow of edema fluid into the alveolar cavity [5, 6]. Despite the great progress has been made in understanding its pathogenesis, the treatment outcome of sepsis-induced ALI remains disappointing, with a high mortality rate ranging from 35% to 40% [7, 8]. Therefore, it is of great importance to investigate the mechanism of sepsis-induced ALI and to exploit available therapeutic targets.

Long non-coding RNAs (lncRNAs), with a length of over 200 nt, which cannot directly encode proteins, has become a hotspot in recent years, which play a pivotal role in regulating many diseases [9, 10]. The regulatory role of lncRNAs in disease-related gene transcription and chromosome modification has been increasingly reported [11, 12]. Research has revealed that lncRNAs can regulate inflammatory mediators. For example, lipopolysaccharide (LPS)-inducible lncRNA Mirt2 has been shown to negatively regulate inflammation [13]. In addition, the lncRNA-FA2H-2-MLKL pathway has an impact on autophagy flux and inflammation in atherosclerosis through mTOR-dependent signals [14]. TUG1, a novel lncRNA (6.7-kb nt) at chromosome 22q12, contributes to photoreceptor cell formation in developing rodent retina [15, 16]. Recent studies have revealed that TUG1 plays a regulatory role in inflammatory response. For example, lncRNA TUG1 reduces LPS-induced apoptosis and inflammation [17].

Moreover, downregulation of lncRNA TUG1 sponges miR-449b-5p by targeting HMGB1 and MMP2, thereby inhibiting ischemia/reperfusion induced apoptosis and inflammation in renal tubular epithelial cells [18]. A previous study has suggested that TUG1 is downregulated in sepsis-induced ALI, but the underlying mechanism remains unexplored [19].

In this study, we demonstrated for the first time that TUG1 can participate in sepsis induced ALI through the miR-494/PDK4 axis, providing a potential target for clinical treatment.

Methods and materials

Sample collection

Eighty patients with sepsis referred to the First People's Hospital of Shangqiu from February, 2017 to February, 2019 were included as the patient group, and fifty healthy individuals who underwent physical examination in our hospital were enrolled as the control group. Peripheral blood was sampled on the day of admission and centrifuged to obtain serum. The remaining samples were stored at -80°C. Inclusion criteria: All the enrolled patients met the diagnostic criteria of sepsis diagnosis according to the Third International Consensus Definitions for Sepsis and Septic Shock [20], with the evidence of infection, sequential organ failure assessment (SO-FA) score ≥ 2 points, body temperature > 38°C or < 36°C, heart rate > 90 beats/min, respiratory rate > 20 beats/min or partial pressure of carbon dioxide (PACO2) < 4.6 kPa, white blood cell count > 12 × 10^9/min or < 4 × 10^9/L, and complete case data. Exclusion criteria: Patients who had recently been treated with immunosuppressive agents or were unwilling to cooperate with the study were excluded. This study was approved by the Medical Ethics Committee of our hospital, and all subjects and their families signed the informed consent. The ethical number was HNLL2104(04).

Cell source

HEK-293 cells (ATCC, Manassas, VA, USA) and mouse pulmonary microvascular endothelial cells (PMVECs, Qincheng Biotech, Shanghai, China) were incubated in a humid incubator with DMEM containing penicillin (100 U/mL), streptomycin (100 μg/mL) and 10% fetal bovine serum (FBS, Gibco) at 37°C with 5% CO_2.

Animal selection

Forty adult male C57BL/6 mice (Vital River, Beijing, China) were exposed to 12-h/12-h dark/light cycles, 22-24°C temperature and 60% humidity, with food and water *ad libitum*.

Cell modeling

miR-494-mimics (5'-UGAAACAUACACGGGAAA-CCUC-3') and the control (mimics-NC, 5'-UUC-UCCGAACGUGUCACGUTT-3') were transfected into PMVECs by liposomes. In addition, the overexpressed TUG1 (TUG1, 5'-GTTATCAGCC-ATGGTACTCTACTTCG-3') synthesized by full-length coding sequence of TUG1 or non-specific sequence (NC) was transferred into adenoviral vectors. When reaching 70-80% confluence, 1 g TUG1-expressing adenovirus or control adenovirus was transfected into PMVECs by ViraPower Adenoviral expression system for 48 hours. The cells were processed with 100 ng/mL LPS 24 hours post-transfection and fixed 6 hours later. In addition, during the rescue experiment, 1 μg TUG1-expressing adenovirus (or control) was co-transfected with miR-494-mimics into PMVECs 24 hours before LPS induction.

Animal modeling

The mice reared adaptively for one week were divided into four groups: sham operation group (Sham), model group (Model), Ad-shNC group (Model + control adenovirus) and Ad-shTUG1 group (Model + TUG1-overexpressing adenovirus). Except for Sham group, the other three groups received cecal ligation and perforation (CLP) according to Matsuda's method. The mice received subcutaneous injection of normal saline for fluid resuscitation immediately after surgery. After the CLP procedure, mice were monitored for survival. Rat lung tissue was collected immediately after death or euthanasia by pentobarbital sodium (200 mg/kg intraperitoneally) at the end of the study. In addition, 20 μL Ad-shTUG1 or Ad-shNC adenoviral solution (10^7 pfu/μL) was injected into the tail vein one week before the establishment of animal model. All adenoviral vectors were designed and constructed by Life Technologies. Ethics approval was granted by the animal ethics committee, and all the operations followed the laboratory animal-guideline for ethical review of animal welfare (2018) [21].

Table 1. Primer sequence

Gene	Upstream sequence (5'-3')	Downstream sequence (5'-3')
TUG1	TAGGAGTGGATGTGTTCTGTAGCA	TGGTCGTGGAATATGGTCAATGAG
miR-494	CTCAACTGGTGTCGTGGAGTCGGCAATTCAGTTGAGGAGGTTTC	ACACTCCAGCTGGGTGAAACATACACGGGA
PDK4	GGAGCATTTCTCGCGCTACA	ACAGGCAATTCTTGTCGCAAA
GAPDH	CAATGACCCCTTCATTGACC	TTGATTTTGGAGGGATCTCG
U6	CTCGCTTCGGCAGCACA	CTCGCTTCGGCAGCACA

qRT-PCR

Total RNA was extracted with Trizol reagent (Invitrogen, Carlsbad, CA), and reverse-transcribed into complementary DNA (cDNA) with the PrimeScript RT kit (Takara, Otsu, Japan) and miRNA reverse transcription kit. Next, the collected cDNA was amplified in ABI 7500 PCR system with the SYBR Premix Ex Taq kit (Takara Biomedical Technology). PCR reactions were conducted in triplicate, and gene alterations were visualized by $2^{-\Delta\Delta Ct}$ method [22]. GAPDH served as internal reference for lncRNA and mRNA, and U6 served as internal reference for the miR (**Table 1**).

Enzyme-linked immunosorbent assay (ELISA)

Changes in TNF-α, IL-1β and IL-6 concentrations in cells and tissues were monitored by ELISA kits (Enzyme-linked Biology, Shanghai, China). Absorbance values at 450 nm were measured with a microplate reader.

Western blot (WB)

The content of protein, isolated with RIPA lysis buffer (Beyotime), was normalized by the bicinchonininc acid assay (Pierce, Rockford, USA). Protein was equally separated (20 μg) by 10% SDS-PAGE and blotted to a PVDF membrane. After sealing at room temperature for 1 hour with 5% skimmed milk, the membrane reacted overnight with anti-PDK4 (Abcam, USA, ab11-0336), Bcl-2 (Abcam, USA, ab32124, 1:1000), Bax (Abcam, USA, ab32503, 1:1000), pro caspase-3 (Abcam, USA, ab32150, 1:1000), cle caspase-3 (Abcam, USA, ab32351, 1:500) and β-catenin (Abcam, USA, ab32572, 1:1000) at 4°C. Afterwards, it was washed with 0.5% TBST buffer and cultured for 1 hour with a secondary antibody (HRP, Abcam, USA, ab6721, 1:5000) at room temperature. The protein bands were recorded with the ECL kit (Millipore, Burlington, MA, USA). At last, quantitative calculation was conducted by ImageJ software.

Hematoxylin and eosin (H&E) staining

After fixation (4% paraformaldehyde, 4°C, 24 h), dehydration, embedding, sectioning (5 μm), and staining (H&E), tissue sections were observed with a BX 51 optical microscope (Olympus Corporation, Tokyo, Japan) at a magnification of 200. The lung tissues of mice were scored in terms of pulmonary interstitial thickening, alveolar edema, neutrophil infiltration, and pulmonary hemorrhage. The higher the score, the more severe the lung injury.

TUNEL

A TUNEL kit (Beyotime, Shanghai, China) was used to evaluate pulmonary cell apoptosis. Lung sections (5 μm) were fixed in 4% paraformaldehyde for 15 minutes at room temperature and cultured with 0.01% Triton X-100 for 10 minutes. Following the addition of TUNEL reaction mixture, the sections were incubated at 37°C for 60 minutes, and then monitored under a fluorescence microscope (Nikon Eclipse Ti-S, Melville, N.Y.). TUNEL positive cells were counted in 12 randomly selected fields.

Flow cytometry (FCM)

Apoptosis was measured by FCM using the Annexin V-FITC kit (BD Biosciences, Franklin Lakes, NJ, USA). The treated-MLE-12 cells were collected, rinsed with ice-cold PBS twice and resuspended in 400 μL 1 × binding buffer. Next, they were incubated for 15 minutes with 10 μL Annexin-V FITC and 5 μL propidium iodide (PI) at 4°C in the dark. Apoptosis rates were analyzed by the FACScan flow cytometer (BD Biosciences).

RNA immunoprecipitation (RIP)

EZ-Magna RIP kit (USA, Millipore) was used to perform RIP. In brief, VIC was harvested and cleaved, and was allowed to react with RIP buffer comprising magnetic beads conjugated with

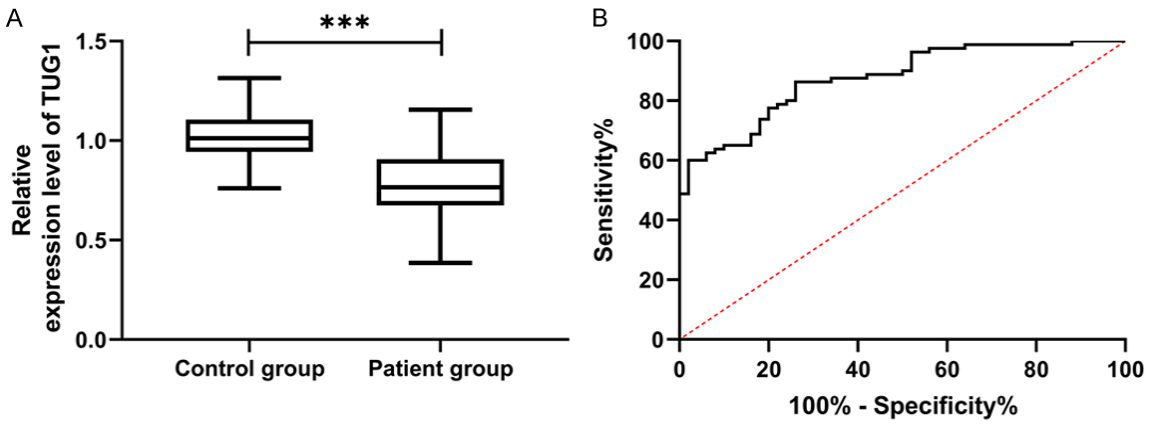

Figure 1. Relative expression of serum TUG1 in sepsis and its diagnostic significance. A. Comparison of serum TUG1 levels between sepsis patients (n=80) and healthy people (n=50) (qRT-PCR). ***$P < 0.001$. B. AUC of TUG1 in diagnosing sepsis is 0.875. When the Youden's index is 60.25%, the optimal specificity is 74.00%, the sensitivity is 86.25%, and the Cut-off is < 0.968 (ROC curve).

human anti-Ago2 antibody or negative control IgG (Millipore). Quantification of TUG1 and miR-494 in the sediment was carried out by qRT-PCR after antibodies were purified using protein A/G beads.

Dual-luciferase reporter (DLR) assay

TUG1 vectors were prepared using full-length TUG1 cDNA cloning into pGL3 DLR vector (Promega, Madison, Wisconsin, USA). HEK-293 cells were intervened with TUG1 vector + NC miRNA (NC group) or TUG1 vector + miR-494-mimics. After a 48-hour incubation (37°C, 95% humidity, 5% CO_2), the relative luciferase activity was measured by the DLR kit (Promega). Renilla luciferases were used to standardize firefly luciferase activity. And the targeting relationship between miR-494 with PDK4 was identified by the same methods mentioned above.

Statistical methods

GraphPad Prism 8 (la Jolla, California, USA) was used for statistical processing. Data were expressed as mean ± SEM. Student's T test was used for comparison between two groups, and analysis of variance (ANOVA) and the Bonferroni post-hoc test were used for comparison among multiple groups. Pearson test was used to identify the correlation between two variables. The diagnostic significance of TUG1 in sepsis was assessed by the receiver operating characteristic (ROC) curve. The death of mice was visualized 72 hours after modeling using a K-M test. Significance was assumed at $P < 0.05$.

Results

Low-expressed lncRNA TUG1 is highly diagnostic in sepsis

We first quantified TUG1 levels by qRT-PCR. Serum TUG1 level decreased in septic patients (**Figure 1A**, $P < 0.001$). Next, ROC curves showed that the area under the curve (AUC) of TUG1 in diagnosing sepsis was > 0.8 (**Figure 1B**), suggesting that TUG1 was involved in sepsis occurrence, and was a promising diagnostic indicator of sepsis.

Overexpressed TUG1 reduced LPS-induced inflammation and apoptosis in PMVECs

We upregulated TUG1 level to understand the role of TUG1 in LPS-treated PMVECs. As shown by qRT-PCR, TUG1 level decreased in LPS and NC groups after LPS induction, and the level in TUG1 group were higher than those in LPS and NC groups, indicating successful transfection (**Figure 2A**, $P < 0.05$). The FCM revealed that compared with LPS and NC groups, the apoptosis was decreased after upregulation of TUG1 (**Figure 2B**, $P < 0.01$). According to WB results, Bax and cle caspase-3 protein levels decreased and Bcl-2 increased after TUG1 upregulation compared with LPS and NC groups (**Figure 2C**, $P < 0.05$). Moreover, the ELISA showed that upregulation of TUG1 led to lower concentrations of TNF-α, IL-1β and IL-6 than LPS and NC groups (**Figure 2D-F**, $P < 0.01$). Therefore, TUG1 upregulation relieved LPS-induced inflammation and attenuated apoptosis in PMVECs.

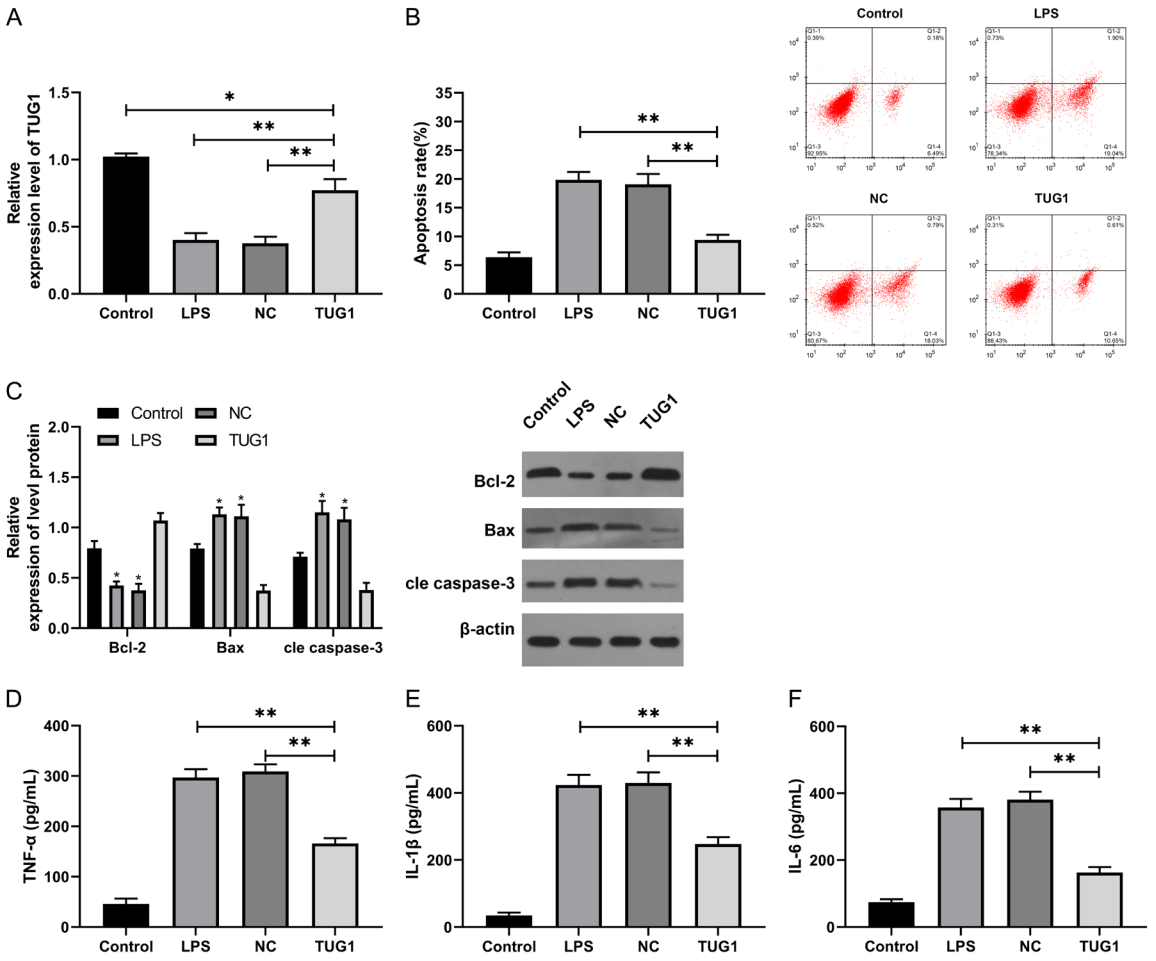

Figure 2. Effect of TUG1 on anti-inflammation and anti-apoptosis in LPS-treated PMVECs. A. Relative expression of TUG1 in LPS-treated PMVECs *in vitro* after upregulation of TUG1 (qRT-PCR). $^{*}P < 0.05$, $^{**}P < 0.01$. (n=3). B. Changes in apoptosis in LPS-treated PMVECs *in vitro* after upregulation of TUG1 (FCM). $^{**}P < 0.01$. (n=3). C. Changes in levels of apoptosis-related proteins in LPS-treated PMVECs *in vitro* after upregulation of TUG1 (WB). $^{*}P < 0.05$ *vs.* TUG1 group, $^{**}P < 0.01$ *vs.* TUG1 group. (n=3). D-F. Changes in TNF-α, IL-1β and IL-6 concentrations in LPS-treated PMVECs *in vitro* after upregulation of TUG1 (ELISA). $^{**}P < 0.01$. (n=3).

TUG1 could regulate miR-494

Competing endogenous RNAs (ceRNAs), as a new mechanism of lncRNAs participating in diseases, have been increasingly studied. To understand the underlying mechanism of TUG1 in sepsis, we predicted downstream binding miRs of TUG1, and found target binding sites between miR-494 and TUG1 (**Figure 3A**). Serum miR-494 was highly expressed in sepsis patients (qRT-PCR, **Figure 3B**, $P < 0.001$); miR-494 was reversely associated with TUG1 (Pearson test, **Figure 3C**). Next, we tried to verify the relationship between miR-494 and TUG1. miR-494-mimics inhibited the luciferase activity of TUG1-WT (DLR assay, **Figure 3D**, $P < 0.05$); Both TUG1 and miR-494 were precipitated by Ago2 antibody (RIP, **Figure 3E**). In addition, UG1 suppressed the overexpression of miR-494 in PMVECs (Rescue experiment, **Figure 3F**, $P < 0.01$). Thus, TUG1 was able to regulate miR-494.

Targeted regulation between miR-494 and PDK4

There is evidence that miRs are involved in sepsis by regulating downstream target genes [23]. In order to understand the mechanism of miR-494 in sepsis, we predicted the downstream target genes. As a result, there were target binding sites between miR-494 and PDK4 (**Figure 4A**). The serum PDK4, with low expression in sepsis (qRT-PCR, **Figure 4B**, $P < 0.001$), was reversely associated with miR-494 and positively associated with TUG1 (**Figure 4C**). miR-494-mimics inhibited the luciferase activity of PDK4-WT (DLR assay, **Figure 4D**, $P <$

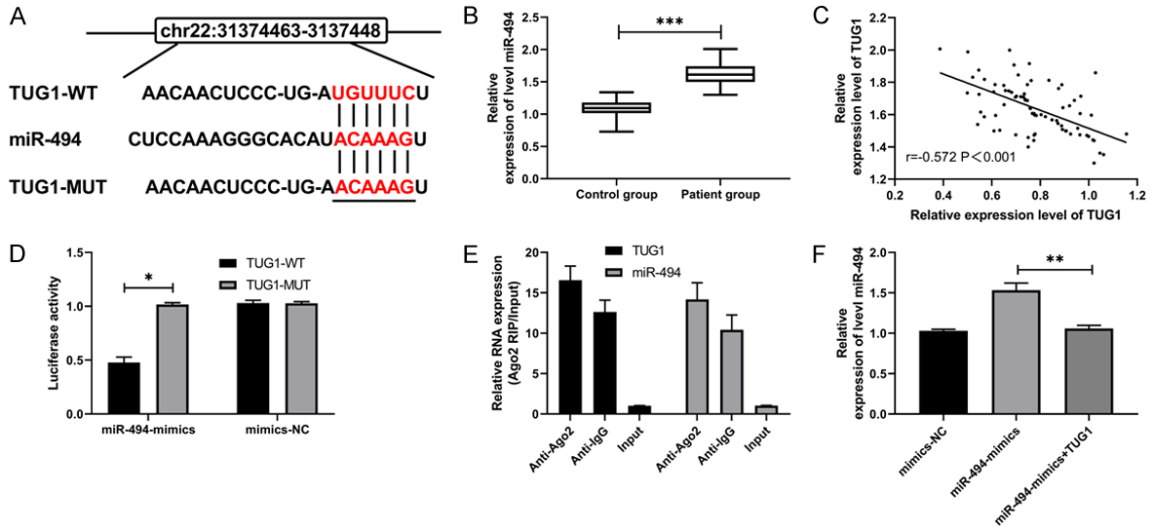

Figure 3. TUG1 could regulate miR-494. A. Binding sites and mutation sites between TUG1 and miR-494. B. Comparison of serum miR-494 levels between sepsis patients (n=80) and healthy people (n=50). ***$P < 0.001$. C. Correlation between the relative expression of TUG1 and miR-494 (Pearson test). (n=80). D. Targeted binding between TUG1 and miR-494 (DLR assay). *$P < 0.05$. (n=3). E. TUG1 could bind with miR-494 (RIP). (n=3). F. Relative expression of miR-494 in PMVECs after co-transfection (qRT-PCR). **$P < 0.01$. (n=3).

0.05). In addition, TUG1 elevated mRNA (qRT-PCR, **Figure 4E**, $P < 0.01$) and protein (WB, **Figure 4F**, $P < 0.05$) levels of PDK4, but its co-transfection with miR-494-mimics inhibited the PDK4 levels.

TUG1 affected LPS-induced apoptosis and inflammation by regulating miR-494/PDK4 axis

We investigated the mechanism of the TUG1/miR-494/PDK4 axis in LPS-treated PMVECs through a rescue experiment. The results revealed that in PMVECs transfected miR-494-mimics alone, the apoptosis rate increased (**Figure 5A**, $P < 0.01$), Bax and cle caspase-3 increased, Bcl-2 and PDK4 decreased (**Figure 5B**, $P < 0.05$), and TNF-α, IL-1β and IL-6 increased (**Figure 5C-E**, $P < 0.05$). However, the above results were reversed after co-transfection of UG1 and miR-494-mimics. Thus, TUG1 reduced LPS-induced apoptosis and inflammation by regulating the miR-494/PDK4 axis.

Upregulation of TUG1 alleviated lung injury, inflammation and apoptosis in septic mice

Animal experiments were conducted at the end of the study. The 72-h survival rates of mice pretreated with Ad-shTUG1 were higher than those in Model and Ad-shNC groups (**Figure 6A**). qRT-PCR indicated that Ad-shTUG1 group had higher TUG1 and PDK4, and lower miR-494 in lung tissues than Model and Ad-shNC groups (**Figure 6B**, **6C**, $P < 0.01$). H&E staining showed that alveolar collapse, alveolar wall thickening, and vascular congestion occurred in Model and Ad-shNC groups, while the lung morphology of mice pretreated by AD-SHUG 1 improved (**Figure 6D**, $P < 0.01$). Furthermore, mice pretreated by Ad-shTUG1 had lower lung injury scores than those in Model and Ad-shNC groups (**Figure 6E**). Upregulation of TUG1 alleviated sepsis-induced ALI in mice (**Figure 6F**, $P < 0.01$). A large number of TUNEL positive cells were seen in Model and Ad-shNC groups, remarkably more than those in lung tissue sections pretreated by Ad-shTUG1 (TUNEL, **Figure 7A**, $P < 0.01$). The results were verified by quantification of apoptosis proteins (WB) (**Figure 7B**, $P < 0.05$). TNF-α, IL-1β and IL-6 levels in lung tissues pretreated by Ad-shTUG1 were lower than those in Model and Ad-shNC groups (ELISA, **Figure 7C-E**, $P < 0.01$). These tests revealed that TUG1 reduced the incidence of sepsis-induced ALI by regulating the miR-494/PDK4 axis.

Discussion

Sepsis is a commonly seen acute and critical illness in clinic, frequently accompanied by ALI [24]. Sepsis-induced ALI has been shown to be associated with higher rates of organ dysfunction and hospitalization mortality than nonsepsis-induced ALI [25]. Herein, we uncovered the low level and the high diagnostic significance of

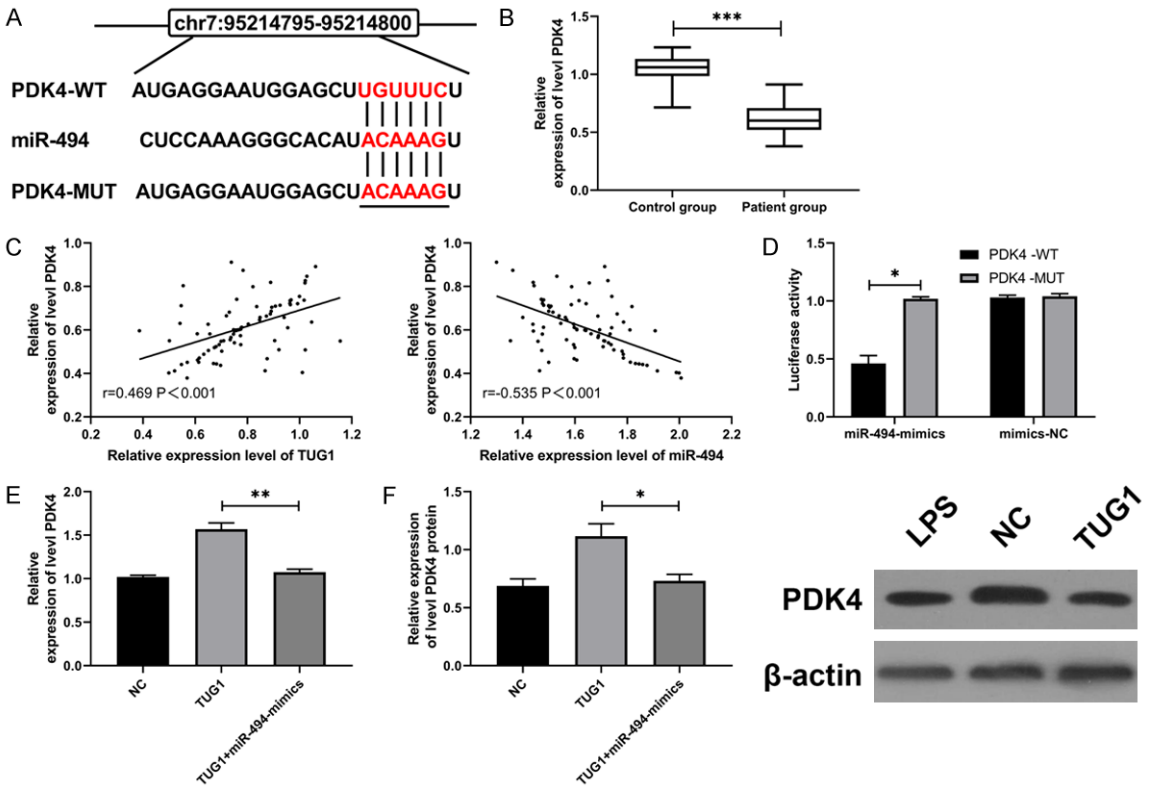

Figure 4. Targeted regulation between miR-494 and PDK4. A. Target binding sites and mutation sites between miR-494 and PDK4. B. Comparison of serum PDK4 levels between sepsis patients (n=80) and healthy people (n=50) (qRT-PCR). ***$P < 0.001$. C. Correlation between PDK4, TUG1 and miR-494 (Pearson test). (n=80). D. Targeted binding between PDK4 and miR-494 (DLR assay). *$P < 0.05$. (n=3). E. Relative mRNA expression of PDK4 in PMVECs after co-transfection (qRT-PCR). (n=3). F. Relative protein expression of PDK4 in PMVECs after co-transfection (WB). **$P < 0.01$. (n=3).

TUG1 in sepsis. Also, upregulation of TUG1 effectively inhibited miR-494 and regulated PDK4, leading to a reduction in inflammation and apoptosis. Therefore, TUG1 is expected to be a feasible therapeutic target.

LncRNAs have outstanding performance in various fields of medicine, especially in regulating immune response and inflammation [26]. For example, lncRNA GATA3-AS1 promotes tumor progression and immune escape in triple negative breast cancer through GATA3 instability and PD-L1 stability [27]. In addition, lncRNA MALAT1 relieves post-stroke inflammation through sponging miR-181c-5p and mediating HMGB1 [28]. TUG1, also known as LINC00080, is known to regulate the pathogenesis of inflammation-related diseases [29]. Serum TUG1 was decreased in both LPS-treated PMVECs and lung tissues of CLP-treated mice in this study. TUG1 overexpression reduced LPS-induced inflammation and apoptosis in PMVECs, as well as relieved CLP-induced lung injury. Thus, we concluded that TUG1 may be a feasible therapeutic target for sepsis-induced ALI.

LncRNAs affect miRs by competing for shared miR response elements (MREs), thereby acting as ceRNAs [30]. We predicted the potential binding miRs of TUG1 to understand the mechanism of TUG1 in sepsis-induced ALI, and found target binding sites between TUG1 and miR-494. miR-494 is associated with inflammation. A high level of miR-494 increased the mortality in middle-aged and elderly patients with sepsis-induced acute kidney injury [31]. Another study reports that miR-494-3p targets PTEN to mediate LPS-induced inflammation in RAW264.7 cells [32]. This study supported that serum miR-494 was high-expressed in septic patients and was reversely associated with TUG1. Moreover, the regulatory effect of TUG1 on miR-494 was confirmed.

PDK4 belongs to the PDK/BCKDK protein kinase family encoding mitochondrial proteins

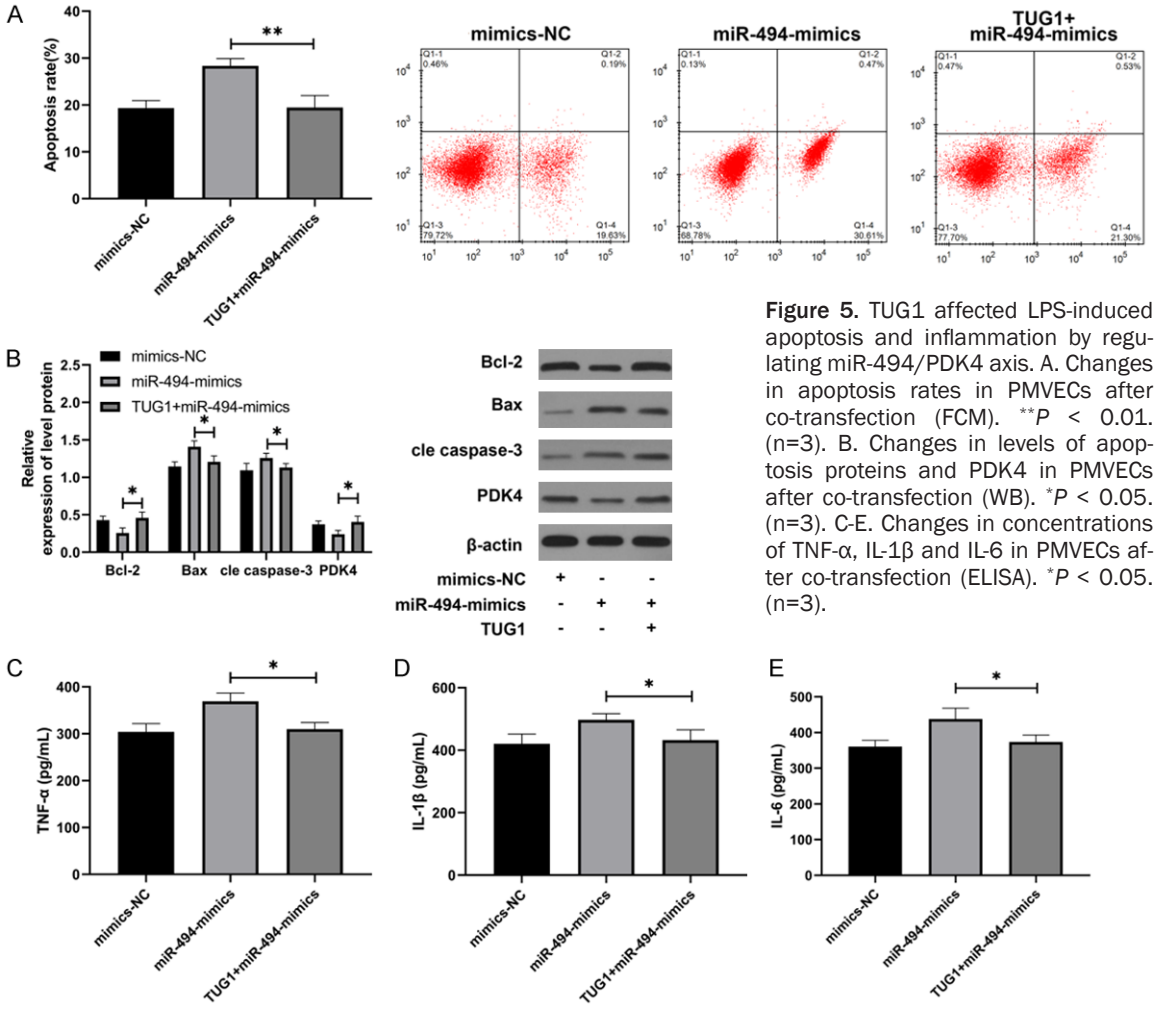

Figure 5. TUG1 affected LPS-induced apoptosis and inflammation by regulating miR-494/PDK4 axis. A. Changes in apoptosis rates in PMVECs after co-transfection (FCM). $^{**}P < 0.01$. (n=3). B. Changes in levels of apoptosis proteins and PDK4 in PMVECs after co-transfection (WB). $^{*}P < 0.05$. (n=3). C-E. Changes in concentrations of TNF-α, IL-1β and IL-6 in PMVECs after co-transfection (ELISA). $^{*}P < 0.05$. (n=3).

with histidine kinase domains [33]. Inflammation increases PDK4 levels in C2C12 cells via the c-jun-N-Terminal Kinase (JNK) pathway [34]. PDK4 is an essential regulator of cellular energy metabolism expressed in experimental models of cancer, diabetes and septicemia [35, 36]. miR-494 shared target binding sites with PDK4. Furthermore, serum PDK4 was low-expressed in sepsis and reversely associated with miR-494, and a targeted relation between them was observed. Therefore, the existence of the TUG1/miR-494/PDK4 axis was determined, but whether this axis exerts a regulatory effect on sepsis-induced ALI remains unknown. The rescue experiment indicated that upregulation of TUG1 reversed the promotion of miR-494-mimics on LPS-induced inflammation and apoptosis in PMVECs. It also improved lung morphology of mice, decreased lung injury score, and enhanced the anti-inflammation and anti-apoptosis of the lung by regulating miR-494/PDK4.

The anti-inflammation and anti-apoptosis mechanisms of the TUG1/miR-494/PDK4 axis in sepsis-induced ALI were discussed (**Figure 8**).

However, there are still limitations in this study. First, relatively few samples were included, so, the diagnostic significance of TUG1 in sepsis is not deeply explored. Second, only HEK-293 cells were studies, while the effect of TUG1 on other lung cells remains unknown. Therefore, we will supplement experiments to verify our results and address these limitations.

To sum up, TUG1 is low-expressed in sepsis, and is a feasible therapeutic target to alleviate the inflammation in sepsis-induced ALI by regulating the miR-494/PDK4 axis.

Disclosure of conflict of interest

None.

Address correspondence to: Peili Chen, Department of Critical Care Medicine, The First People's Hospital

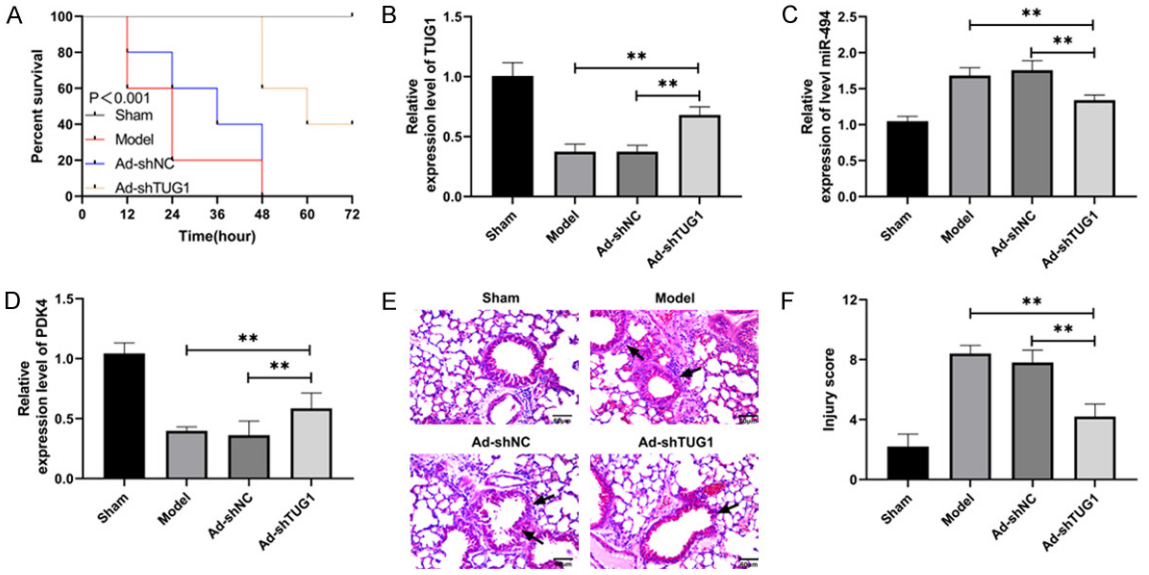

Figure 6. Upregulation of TUG1 alleviated lung injury in septic mice. A. Effect of TUG1 upregulation on 72-h survival of septic mice (K-M survival curve). (n=10). B-D. Relative mRNA expression of TUG1, miR-494 and PDK4 in CLP-induced mouse model (qRT-PCR, $^{**}P < 0.01$). (n=10). E. Lung injury in the CLP-induced mouse model (H&E staining). (n=10). F. Lung injury scores in the CLP-induced mouse model. $^{**}P < 0.01$. (n=10). Note: Insertional area of tissue injury and inflammation inflow.

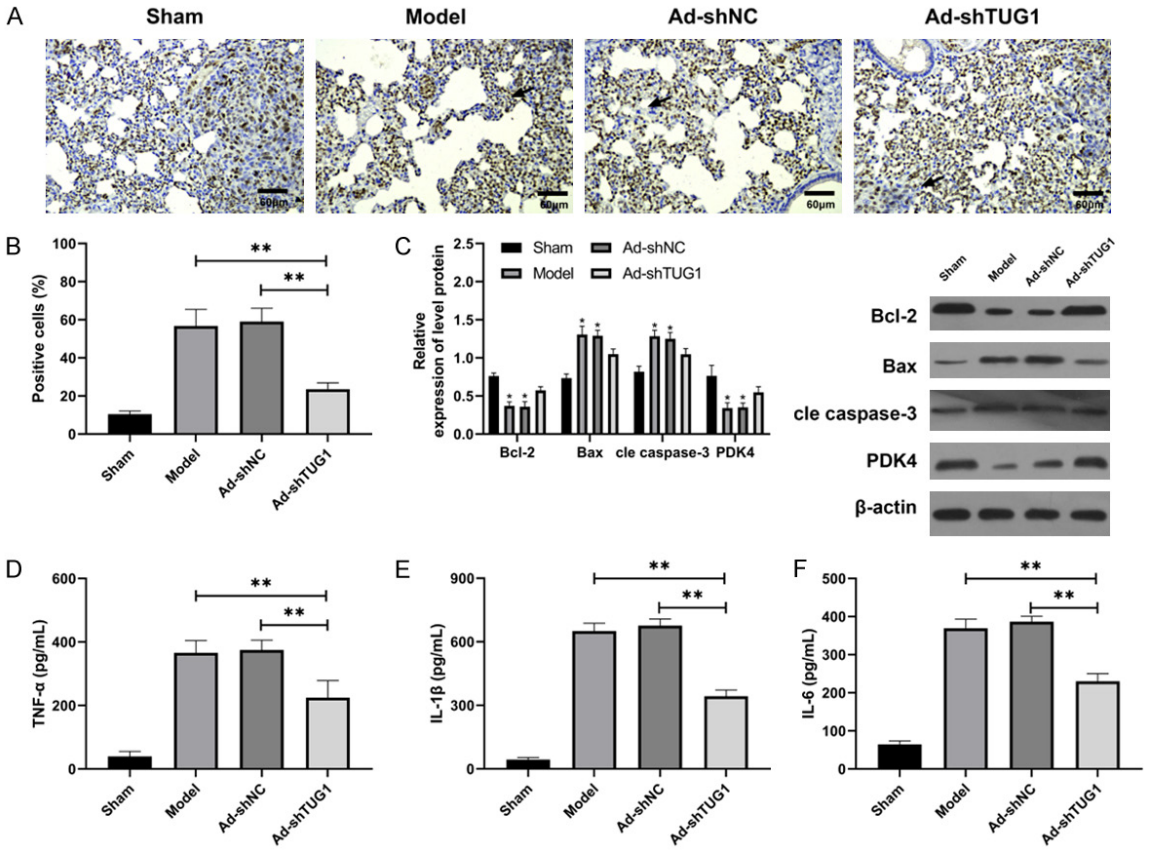

Figure 7. Upregulation of TUG1 alleviated lung inflammation and apoptosis in septic mice. A, B. Apoptosis in septic mice treated with Ad-shTUG1 (TUNEL). $^{**}P < 0.01$. (n=10). C. Changes in levels of apoptosis-related proteins and PDK4 in septic mice treated with Ad-shTUG1 (WB). $^{*}P < 0.05$ *vs.* Ad-shTUG1 group, $^{**}P < 0.01$ *vs.* Ad-shTUG1 group.

(n=10). D-F. Changes in concentrations of TNF-α, IL-1β and IL-6 in septic mice treated with Ad-shTUG1 (ELISA). $^{**}P < 0.01$. (n=10). Note: Black arrows mark the mouse alveolar congestion, alveolar stroma and alveolar cell infiltration.

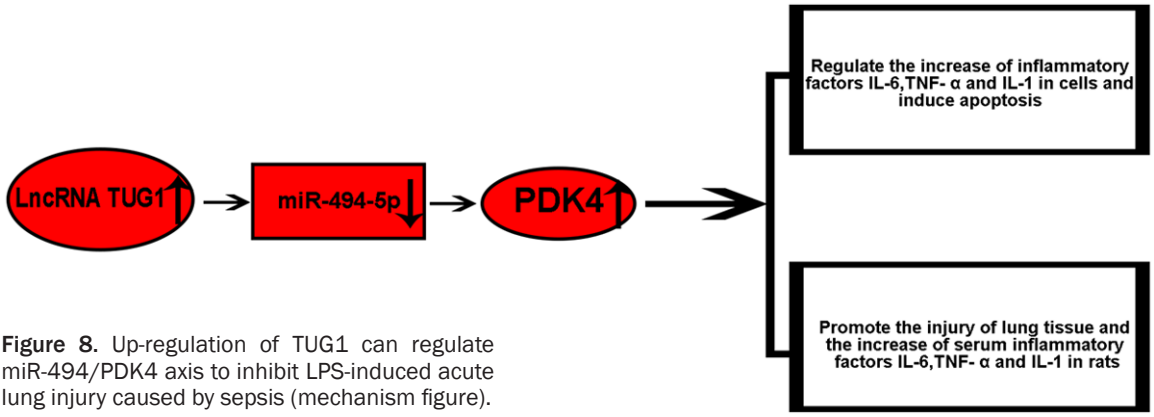

Figure 8. Up-regulation of TUG1 can regulate miR-494/PDK4 axis to inhibit LPS-induced acute lung injury caused by sepsis (mechanism figure).

of Shangqiu, 292 Kaixuan South Road, Suiyang District, Shangqiu 476100, Henan Province, China. Tel: +86-13837088832; E-mail: Peili88832@163.com

References

[1] van der Poll T, van de Veerdonk FL, Scicluna BP and Netea MG. The immunopathology of sepsis and potential therapeutic targets. Nat Rev Immunol 2017; 17: 407-420.

[2] Nowill AE, Fornazin MC, Spago MC, Dorgan Neto V, Pinheiro VRP, Alexandre SSS, Moraes EO, Souza G, Eberlin MN, Marques LA, Meurer EC, Franchi GC Jr and de Campos-Lima PO. Immune response resetting in ongoing sepsis. J Immunol 2019; 203: 1298-1312.

[3] Zhao H, Chen H, Xiaoyin M, Yang G, Hu Y, Xie K and Yu Y. Autophagy activation improves lung injury and inflammation in sepsis. Inflammation 2019; 42: 426-439.

[4] Mehaffey JH, Charles EJ, Schubert S, Salmon M, Sharma AK, Money D, Stoler MH, Laubach VE, Tribble CG, Roeser ME and Kron IL. In vivo lung perfusion rehabilitates sepsis-induced lung injury. J Thorac Cardiovasc Surg 2018; 155: 440-448, e2.

[5] Liu Y, Mu S, Li X, Liang Y, Wang L and Ma X. Unfractionated heparin alleviates sepsis-induced acute lung injury by protecting tight junctions. J Surg Res 2019; 238: 175-185.

[6] Bajwa RPS, Mahadeo KM, Taragin BH, Dvorak CC, McArthur J, Jeyapalan A, Duncan CN, Tamburro R, Gehred A, Lehmann L, Richardson P, Auletta JJ and Woolfrey AE. Consensus report by pediatric acute lung injury and sepsis investigators and pediatric blood and marrow transplantation consortium joint working committees: supportive care guidelines for management of veno-occlusive disease in children and adolescents, part 1: focus on investigations, prophylaxis, and specific treatment. Biol Blood Marrow Transplant 2017; 23: 1817-1825.

[7] Xia W, Zhang H, Pan Z, Li G, Zhou Q, Hu D and Liu Y. Inhibition of MRP4 alleviates sepsis-induced acute lung injury in rats. Int Immunopharmacol 2019; 72: 211-217.

[8] Hendrickson CM and Matthay MA. Endothelial biomarkers in human sepsis: pathogenesis and prognosis for ARDS. Pulm Circ 2018; 8: 2045894018769876.

[9] Ferre F, Colantoni A and Helmer-Citterich M. Revealing protein-lncRNA interaction. Brief Bioinform 2016; 17: 106-116.

[10] Yang Q, Wan Q, Zhang L, Li Y, Zhang P, Li D, Feng C, Yi F, Zhang L, Ding X, Li H and Du Q. Analysis of LncRNA expression in cell differentiation. RNA Biol 2018; 15: 413-422.

[11] Wieczorek E and Reszka E. mRNA, microRNA and lncRNA as novel bladder tumor markers. Clin Chim Acta 2018; 477: 141-153.

[12] Zhang P, Cao L, Zhou R, Yang X and Wu M. The lncRNA Neat1 promotes activation of inflammasomes in macrophages. Nat Commun 2019; 10: 1495.

[13] Du M, Yuan L, Tan X, Huang D, Wang X, Zheng Z, Mao X, Li X, Yang L, Huang K, Zhang F, Wang Y, Luo X, Huang D and Huang K. The LPS-inducible lncRNA Mirt2 is a negative regulator of inflammation. Nat Commun 2017; 8: 2049.

[14] Guo FX, Wu Q, Li P, Zheng L, Ye S, Dai XY, Kang CM, Lu JB, Xu BM, Xu YJ, Xiao L, Lu ZF, Bai HL, Hu YW and Wang Q. The role of the LncRNA-FA2H-2-MLKL pathway in atherosclerosis by regulation of autophagy flux and inflammation through mTOR-dependent signaling. Cell Death Differ 2019; 26: 1670-1687.

[15] Tian L, Zhao ZF, Xie L and Zhu JP. Taurine up-regulated 1 accelerates tumorigenesis of co-

lon cancer by regulating miR-26a-5p/MMP14/p38 MAPK/Hsp27 axis in vitro and in vivo. Life Sci 2019; 239: 117035.
[16] Lin YH, Wu MH, Huang YH, Yeh CT, Cheng ML, Chi HC, Tsai CY, Chung IH, Chen CY and Lin KH. Taurine up-regulated gene 1 functions as a master regulator to coordinate glycolysis and metastasis in hepatocellular carcinoma. Hepatology 2018; 67: 188-203.
[17] Hu L, Ye H and Liao J. LncRNA TUG1 reverses LPS-induced cell apoptosis and inflammation of macrophage via targeting MiR-221-3p/SPRED2 axis. Biosci Biotechnol Biochem 2020; 84: 2458-2465.
[18] Xu Y, Niu Y, Li H and Pan G. Downregulation of lncRNA TUG1 attenuates inflammation and apoptosis of renal tubular epithelial cell induced by ischemia-reperfusion by sponging miR-449b-5p via targeting HMGB1 and MMP2. Inflammation 2020; 43: 1362-1374.
[19] Wang L, Zhong Q, Feng Y, Tang X, Wang Q, Zou Y and Duan J. Long noncoding RNA TUG1 is downregulated in sepsis and may sponge miR-27a to downregulate tumor necrosis factor-alpha. J Int Med Res 2020; 48: 300060520910638.
[20] Singer M, Deutschman CS, Seymour CW, Shankar-Hari M, Annane D, Bauer M, Bellomo R, Bernard GR, Chiche JD, Coopersmith CM, Hotchkiss RS, Levy MM, Marshall JC, Martin GS, Opal SM, Rubenfeld GD, van der Poll T, Vincent JL and Angus DC. The third international consensus definitions for sepsis and septic shock (Sepsis-3). JAMA 2016; 315: 801-810.
[21] MacArthur Clark JA and Sun D. Guidelines for the ethical review of laboratory animal welfare People's Republic of China National Standard GB/T 35892-2018 [Issued 6 February 2018 Effective from 1 September 2018]. Animal Model Exp Med 2020; 3: 103-113.
[22] Livak KJ and Schmittgen TD. Analysis of relative gene expression data using real-time quantitative PCR and the 2(-Delta Delta C(T)) method. Methods 2001; 25: 402-408.
[23] Shen Y, Yu J, Jing Y and Zhang J. MiR-106a aggravates sepsis-induced acute kidney injury by targeting THBS2 in mice model. Acta Cir Bras 2019; 34: e201900602.
[24] Rowe TA and McKoy JM. Sepsis in older adults. Infect Dis Clin North Am 2017; 31: 731-742.
[25] Sevransky JE, Martin GS, Shanholtz C, Mendez-Tellez PA, Pronovost P, Brower R and Needham DM. Mortality in sepsis versus non-sepsis induced acute lung injury. Crit Care 2009; 13: R150.
[26] Huang-Fu N, Cheng JS, Wang Y, Li ZW and Wang SH. Neat1 regulates oxidized low-density lipoprotein-induced inflammation and lipid uptake in macrophages via paraspeckle formation. Mol Med Rep 2018; 17: 3092-3098.
[27] Zhang M, Wang N, Song P, Fu Y, Ren Y, Li Z and Wang J. LncRNA GATA3-AS1 facilitates tumour progression and immune escape in triple-negative breast cancer through destabilization of GATA3 but stabilization of PD-L1. Cell Prolif 2020; 53: e12855.
[28] Cao DW, Liu MM, Duan R, Tao YF, Zhou JS, Fang WR, Zhu JR, Niu L and Sun JG. The lncRNA Malat1 functions as a ceRNA to contribute to berberine-mediated inhibition of HMGB1 by sponging miR-181c-5p in poststroke inflammation. Acta Pharmacol Sin 2020; 41: 22-33.
[29] Zhang Y, Gu M, Ma Y and Peng Y. LncRNA TUG1 reduces inflammation and enhances insulin sensitivity in white adipose tissue by regulating miR-204/SIRT1 axis in obesity mice. Mol Cell Biochem 2020; 475: 171-183.
[30] Karreth FA and Pandolfi PP. ceRNA cross-talk in cancer: when ce-bling rivalries go awry. Cancer Discov 2013; 3: 1113-1121.
[31] Lin Y, Ding Y, Song S, Li M, Wang T and Guo F. Expression patterns and prognostic value of miR-210, miR-494, and miR-205 in middle-aged and old patients with sepsis-induced acute kidney injury. Bosn J Basic Med Sci 2019; 19: 249-256.
[32] Zhang S, He K, Zhou W, Cao J and Jin Z. miR4943p regulates lipopolysaccharide-induced inflammatory responses in RAW264.7 cells by targeting PTEN. Mol Med Rep 2019; 19: 4288-4296.
[33] Guda MR, Asuthkar S, Labak CM, Tsung AJ, Alexandrov I, Mackenzie MJ, Prasad DV and Velpula KK. Targeting PDK4 inhibits breast cancer metabolism. Am J Cancer Res 2018; 8: 1725-1738.
[34] Park H and Jeoung NH. Inflammation increases pyruvate dehydrogenase kinase 4 (PDK4) expression via the Jun N-Terminal Kinase (JNK) pathway in C2C12 cells. Biochem Biophys Res Commun 2016; 469: 1049-1054.
[35] Pin F, Novinger LJ, Huot JR, Harris RA, Couch ME, O'Connell TM and Bonetto A. PDK4 drives metabolic alterations and muscle atrophy in cancer cachexia. FASEB J 2019; 33: 7778-7790.
[36] Park BY, Jeon JH, Go Y, Ham HJ, Kim JE, Yoo EK, Kwon WH, Jeoung NH, Jeon YH, Koo SH, Kim BG, He L, Park KG, Harris RA and Lee IK. PDK4 deficiency suppresses hepatic glucagon signaling by decreasing cAMP levels. Diabetes 2018; 67: 2054-2068.